INTERNATIONAL BUILDING PERFORMANCE SIMULATION ASSOCIATION ENGLAND

Proceedings of BSO-V 2020
5th Building Simulation and Optimization Virtual Conference
21-22 September 2020
Loughborough, UK

Parameters identification of grey-box building energy model through Bayesian calibration

Victor Marty-Jourjon[1], Thomas Berthou[1], Pascal Stabat[1]
[1]Mines Paristech, PSL Research University, CES centre d'efficacité énergétique des systèmes

Abstract

This study discusses the physical interpretability of the grey-box models parameters. This physical interpretability allows robust calibration of building models parameters with Bayesian methods, and could help to assess scenario of retrofitting, and detect building energy drift. However, since these models simplify the physical complexity, the link between the physical characteristics and the model parameters is not straightforward, and can significantly vary with structure of the RC model. Five RC models have been selected and calibrated using a Bayesian approach with a training data set issued from a typical office building simulated with TRNSYS. The calibrated parameters are compared to the theoretical physical values modeled in TRNSYS. The results discuss the parameters of thermal resistance and suggest that at this stage, only the global resistance can be identified. Issues of correlation between the parameters are highlighted and a set of robust models is proposed.

Introduction

In the context of global warming, buildings appear to be an indispensable lever for action as they represent over one-third of the final energy consumption and nearly 40% of total direct and indirect CO2 emissions IEA (2020). Two main kinds of actions can be undertaken: the global need of energy can be reduced through retrofitting and sobriety; and the dynamics of the demand can be modified to better follow energy production patterns (demand response); for example by using the thermal capacities of buildings to shift a part of the energy demand by a few hours.

Within this context, building energy model can be used to simulate scenarios of retrofitting and flexibility. Such actions can also be evaluated within the framework of the International Performance Measurement and Verification Protocol EVO (2010) by analysing the gap between the energy use given by a pre-retrofit and a post-retrofit model.

The information used to generate building energy models can be classified in two categories: the building information data, such as wall resistances and thermal capacities; and the operation data, such as inside temperature and energy consumption measurements.

To consider both kinds of information, a Bayesian calibration method can be used. With this method, the building information is taken into account through the prior probabilities, and the operation data are used as the calibration data to calculate the posterior probabilities. This method allows using all available information and prevents from over-fitting as the prior probabilities act as a penalisation term Martin (2018). Therefore, the predicted data and the estimated parameters associated to probability distribution are more robust than with a determinist non-penalised identification method.

Different types of models can be used in this method. Firstly, the detailed physical models, such as TRNSYS or EnergyPlus, can be applied. Such models can consider a large amount of physical phenomena. However, a lot of building data is required which can be difficult to collect in a reasonable amount of time. Additionally, these models require heavy calculations, which are unsuited for Bayesian calibration method. Secondly, purely statistic models can be applied such as Artificial Neural Networks (ANN) Wang and Chen (2019). These models can be trained with onsite measurements; however, they cannot directly consider building information such as wall resistance.

The grey-box models, or RC models, representing the building component with resistances (R) and capacities (C), can be seen as a trade-off between the detailed models and the statistic models. Although, such models can be used as statistic models with a weak or not existent link between the parameters and the physical properties, they are built from physical analogies and the parameters are often considered as physically interpretable. Besides, these models have a low computational cost. However, to efficiently conduct a Bayesian calibration of such models, a better comprehension of the link between the parameter values of the models and the physical properties of the buildings is required. Since, these models simplify the physical complexity, the link between the physical characteristics and the

Table 1: Review of the mains contributions to the issue of physical interpretation of RC-model parameters

Authors	**Models**	**Case study**	**Training period**	**Identification method**	**Contributions to the identification issue**
Brastein et al. (2018)	R3C2	Experimental setup of 9.4 m^3	November and December	- Constrained Optimization BY Linear Approximation (COBYLA) - Data time step: 10 minutes	The paper claims that in order to assign a physical interpretation to grey-box model parameters, the estimated parameters have to converge independently of the initial conditions and different datasets. Thus they investigate the parameter convergence of a R3C2 model and conclude that for physical interpretation the parameters related to the thermal resistance of windows and doors need to be fixed.
Wang et al. (2019)	R3C2	- Real case - Individual dwelling	30 days of January	- Prediction error method (PEM) - Data time step: 30 minutes	The model R3C2 is selected amongst 4 models for its prediction ability and the physical plausibility of the parameters.
Harb et al. (2016)	1R1C 3R2C 4R2C 8R3C	- Real case - Office building of 33 140 m2	Approx. 1 month between January and March.	- Interior Point algorithm - Data time step: 60 minutes	The authors define boundaries with respect to the building physics so that the identified parameters out of these boundaries are considered not plausible. Only the calibrated 1R1C and 4R2C models are considered physically plausible by the authors.
Madsen and Holst (1995)	R3C2	- Real case - Individual dwelling	October 10-14	Maximum likelihood method with Kalman filter	The identified parameters are compared with the physically evaluated parameters. The global resistances match well (between 10 to 20% of error). The total heat capacity presents around 30% of error.
Raillon and Ghiaus (2018)	R4C3	- Real case. - Individual dwelling	14 days of April and May	- Posterior probability sampling with Kalman filter - Data time step: 10 minutes	The posterior distributions are compared against the building physical parameters. Only the envelope thermal resistance turns out to be correctly identified.
Reynders et al. (2014)	R1C1 R3C2 R4C3 R6C2 R8C5	Detailed simulation of two detached single family dwellings	5 sets of data between February and June	- Maximum likelihood estimation (MLE) - Data time step: 10 minutes	The parameters are compared to the theoretical physical properties implemented in the detailed simulations. The models of orders three and four display a good identifiability of the UA-value of opaque envelope, the indoor air capacity and the ventilation losses. For the lumped capacity of envelope, internal walls and floors, the discrepancy is higher (around 20%) and the results are less consistent.
Hedegaard and Petersen (2017)	2R2C 4R3C 3C2C 4R3Cw	Detailed simulations of two apartments	4 sets of two weeks data between November and February	- Unknown method - Data time step: 1 minute	Identified parameters were compared to estimates from calculation methods described in relevant standards. All the tested models identify precisely the overall heat loss coefficient and the short time constant (air and furniture). Besides, both second order and third order models are capable of yielding consistent estimates of the effective thermal mass (slightly overestimated by 10-32%). However, the estimated parameters related to infiltration and transmission heat losses were found to be highly inconsistent across all models.

model parameters is not straightforward, and can significantly vary with structure of the RC model. This issue has seldom been studied in the literature. A better understanding of this link would allow defining more pertinent prior probabilities and hence, building more robust models with better predictive capacities. Additionally, identifying the physical properties of buildings through Bayesian calibration of grey box models would help to assess scenario of retrofitting, and detect operation or construction deviations.

Bayesian calibration with RC models can be particularly interesting at district scale. At this scale, the models must have a low comptutional cost as many buildings have to be simulated. In addition, at this scale, as the available data might be few and heterogenous, this approach would allow using operation data as well as databases. District turns out to be a relevant scale to undertake actions of retrofitting or flexibility. Multiple demand response schemes of individual buildings can be aggregated and global actions of retrofitting can be conducted. During the last years, several urban district models using RC models have been developed Berthou et al. (2015) Fonseca et al. (2016).

The main literature contributing to this issue of the physical interpretability of RC models parameters is summarized in Table 1. Four publications have been found trying to compare identified parameters with corresponding physical estimates; the others only assess the physical plausibility of the parameters. Most of the models succeed to identify the global resistance of the building. For the other parameters, the results are less consistent. Only Reynders et al. (2014) obtain consistent results for the resistance related to the infiltration and ventilation. The short time constant (air, furniture) is identified by Reynders et al. (2014) and Hedegaard and Petersen (2017). Identifying the lumped capacity of the envelope, internal walls and floors is also not straightforward as only one part of the total physical thermal capacity might be activated. Reynders et al. (2014) consider as the theoretical value an estimate of the thermal mass of the materials within the insulation layer; they find a good agreement with the estimated parameters. Madsen and Holst (1995) proposed a model for the case where the capacity in the outer wall is of minor importance. Hence, the long term capacity is estimated from the floor thermal capacity. This estimate turns out to be higher than the identified value (around 30% of error). Hedegaard and Petersen (2017) found a good agreement between the effective mass capacity ISO 13786 and the identified time constant multiplied with the total heat loss coefficient.

A general method does not emerge from this literature and the results show an important discrepancy. This paper brings new insights to this issue. The identification problem of grey-box models is studied through data of an office building, generated with TRNSYS. Various RC models are considered. A Bayesian approach is used for identification. Therefore, the consistency of the results can be more easily evaluated through the convergence analysis of the sample chains. The correlation between the calibrated parameters can also be observed. At last, the fitting of the models with the training and testing data is discussed.

Table 2: Characteristic of the office buildings modelled on TRNSYS

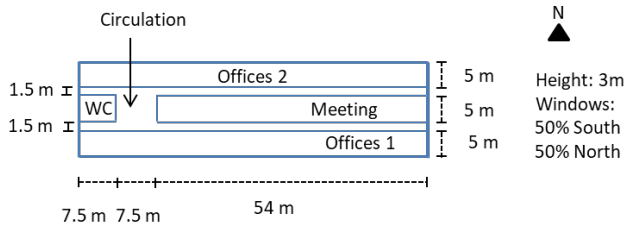

Geometry	(Top view of one floor)
Uwalls	0.8 W/m.K (Internal insulation)
Uwindows	3 W/m.K
Uroof	0.6 W/m.K (Internal insulation)
Zone capacitance	29 000 kJ/K (8*Air volume)
Thermal mass	Floors: 262 807 kJ/K (0.1 m of concrete) Wall 143 591 kJ/K (0.13 m of concrete) Roof 262 807 kJ/K (0.1 m of concrete)
Interior convection	3 W/m.K
Exterior convection	18 W/m.K
Occupation	Offices zones & Meeting zones: 9m/pers, 80 W/pers Schedule: Offices zones: 6h-18h Schedule: Meeting rooms: 9h-10h & 14h-17h
Appliance Load	Office zones: 15 W/m Schedule: 00h-7h: 18% ->7h-10h: linear ->10h-17h : 80 % ->17h-20h: linear ->20h-24h: 18 %
Light load	15 W/ m Schedule: Function of occupation and solar radiations
Ventilation	Office zones: 0.7 vol/h, Meeting room: 2.85 vol/h Schedule: Occupation
Infiltration	0.2 1/h Schedule : Constant
Solar radiation	Transmittance : 0.77, Absorbance: 0.6 Meteonorm (Paris)
Heating power max	300 kW

Case study

To assess the physical meaning of grey-box model parameters, a fully controlled case, an office building modeled on TRNSYS, is considered. The solicitations (outdoor temperature, solar radiation, ventilation and other internals gains), the heating power and the indoor temperature in every zone of the building

are perfectly known. A typical office building Alessandrini et al. (2003) constituted of 5 identical floors separated in 5 zones has been chosen.

The characteristics of the building are detailed in Table 2. Three weeks of winter are considered for the calibration period. The three following weeks are used as the testing period. For the testing period, the scheme of temperature set point has been slightly modified to assess the robustness of the model: the set point is fixed at 23°C between 3am to 8am, so that a part of the morning peak energy demand is shifted.

Models studied

Many RC models have been proposed in the literature. For each model, some parameters can be fixed or merged. Thus, a large set of models with different properties of identifiability, fitting and prediction can be used. A set of five RC models has been selected by the authors: the model described in the norm ISO 13790 and 4 models derived from the model R6C2 presented in Berthou et al. (2014).

The model ISO has been specifically created to be used with physical parameters and has been assessed under the BESTEST method Roujol et al. (2003). The model R6C2 has recently shown good results of fitting for an office building Berthou et al. (2014). Besides, both the models R6C2 and R5C1 are used in a tool for energy demand simulation at district scale, respectively SMART-E Berthou et al. (2015) and City Energy Analyst Fonseca et al. (2016). To cover a larger panel, four additional models derived from the model R6C2 have been considered.

The model R6C2 is presented in Figure 1 as a R5C1. The two resistances of infiltration and heat loss through the windows have been merged into a single resistance Rv, since they have very similar effect on the model. Re and Ri are the resistances of convection. Re considers the surface of the opaque envelope; and Ri considers in addition the surfaces of the floors. Rw1 and Rw2 represent the resistances of conduction of the walls (including the roof). The thermal capacity outside of insulation layer is not considered, all the thermal mass within the insulation layer (roof, wall and floor) is attributed to Cw. Thus, 95% of the resistance Rw is attributed to Rw2 while only 5% is given to Rw1. The capacity, Cw is related to thermal mass of the walls (including roof) and the floor, and Ci refers to the quick dynamic of the air volume. Three thermal fluxes are considered. The internal gains (appliance, lighting and metabolism) are separated in a convective part passed through S1 and a radiative part passed through S2. The power of the heating system is supposed to be convective and is thus passed through S1. At last, the solar radiation heating the outside opaque surfaces is passed through S3 and the solar radiation entering the office through the windows is passed through S2.

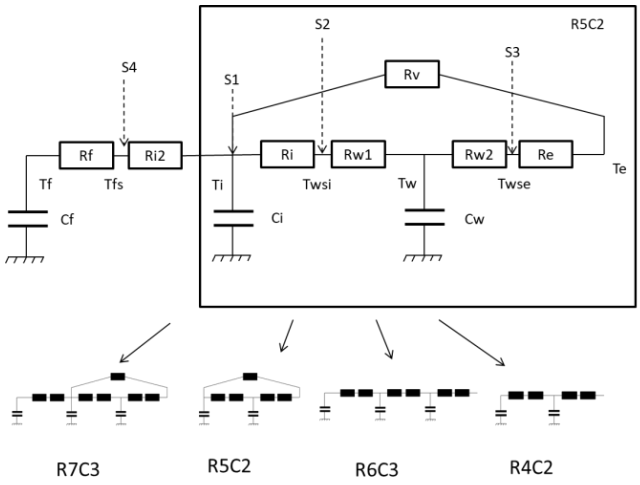

Figure 1: Schematics of the model R7C3 and its derivatives

An extension of the R5C2 has also been considered in this study by adding to the model a capacity Cf and a resistance Rf related to the thermal mass of the floor, resulting in a third order model: R7C3 (Figure 1). Ri2 is the resistance of convection associated to the floor surface; Ri considers only the interior surfaces of the opaque envelope. The thermal capacity outside of insulation layer is modelled through Cw. Hence, the resistance of the opaque envelope Rw is mainly distributed to Rw1 (95%); the remaining 5% of Rw is attributed to Rw2. The whole inner thermal mass is modelled through Cf. An additional flux S4 including the inner solar radiation and 50% of the other radiative internal gain, is considered.

Two more derivatives R4C2 and R6C2 are included to the study, corresponding to the models R5C2 and R7C3 where the resistance Rv has been aggregated to Rw (Figure 1). The scheme of R5C1 presented

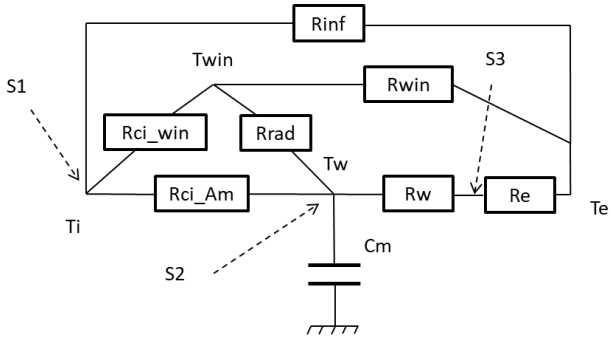

Figure 2: Detailed representation of the model ISO 13790

in ISO 13790 can be seen as a mathematical simplification the model presenter in Figure 2. The main characteristic is that the node related to the heavy walls (Tw), is linked to the air node Ti, and the inner windows surface node Twin, respectively through a resistance of convection and a resistance of

radiation, considering an exchange surface Am. Am and Cm can be calculated according to ISO 13786. As in the others models, Rv will be considered as the equivalent resistance of the infiltration and the heat loss through the windows. When Rv is calibrated, the rate of distribution between Rinf and Rwin is fixed.

Finally, five models studied are R7C3, R5C2, ISO, R6C3 and R4C2. It is not possible to calibrate all the parameters, as high correlations between the resistances will make the convergence difficult. In all the proposed models, the calibrated parameters are Ci, Cf, Cw, Rf, Rv, and Rw. The resistances of convection and radiation have been fixed. A sensibility analysis has been conducted to verify that Rv and Rw are the most influencing resistances. The capacities are calibrated, but relating these capacities with the physical properties would require another specific study. Thus, in this study only the physical interpretability of the resistance Rv and Rw is discussed.
Since the first results have shown a high correlation between the parameters Rv and Rw, two new parameters have been introduced: Rg representing the global equivalent resistance of Rw and Rv associated in parallel, and Rg_rate characterizing the distribution of Rg between Rw and Rv such as:

$$\begin{aligned} 1/Rw &= 1/Rg \times Rg\_rate \\ 1/Rv &= 1/Rg \times (1 - Rg\_rate) \end{aligned} \tag{1}$$

Thus, three cases are studied:

- case 1: Rv and Rw are calibrated,
- case 2: Rg and Rg_rate are calibrated,
- case 3: Rg is calibrated and Rg_rate is fixed.

For the model R6C3 and R4C2, Rv and Rw are aggregated through Rg, and thus only the case 3 can be considered. In the following, we will refer to the different cases as different models. The Table 3 resumes the resulting 11 calibrated models. In this table, for each model, the presented parameters are associated to one of the following categories:

- the calibrated parameters (green)
- the indirectly calibrated parameters (orange)
- the fixed parameters (red)
- the parameters not defined for the considered model (gray)

Each line correspond to one model (for example : the line 3 presents the indicators of the calibrated model R5C2 where Rg is calibrated (green), Rg_rate is fixed (red) and Rw and Rv are indirectly calibrated through the calibration of Rg (orange). The indicators are described in the following part. The main results are discussed in the corresponding section.

Calibration method

The models are calibrated with a Bayesian method. The likelihood function is presented in (2). The calibration dataset is the mean hourly interior temperature issued from the TRNSYS model. The power, the solar radiation and the other internal gains are considered as inputs in the RC model. As the TRNSYS model considers multiple zones with different temperatures, the mean interior temperature is weighed by the air volume of each zone. The prior probabilities are chosen flat as the objective is to study the link between the parameters and the physical properties without a priori. The posterior probability function is estimated with a Markov Chain Monte Carlo (MCMC) slice sampling method Neal (2003). Three chains of sample are computed in parallel with 1500 draws and 300 burn-in points by chains.

$$\begin{aligned} L = P(D \mid \eta(\theta)) &= \prod_{n=1}^{N} P(D_n \mid \eta_n(\theta)) \\ &= \prod_{n=1}^{N} \frac{1}{\sigma\sqrt{2\pi}} e^{\frac{1}{2}\left(\frac{\eta_n(\theta) - D_n}{\sigma}\right)^2} \end{aligned} \tag{2}$$

D : Calibration dataset
θ : Calibrated parameters
$\eta(\theta)$: Simulated temperature
n : Time step

A computer with a 2.7 GHz processor and 32GB of RAM has been used. The models are coded in python and compiled in C language with the package Cython. The compiled models take around 0.005s to simulate 3 weeks with a time step of 10min. The sampling is conducted with the python package pymc3. Sampling the 3 chains in parallel takes around 15 min.

For each calibration, various indicators are given. These indicators are listed below:

- *The normalized mean calibrated values*
  It indicates mean values of the posterior distributions of the calibrated parameters normalized by the corresponding physical properties of the TRNSYS model. Thus, a value close to 1 indicates a good identifiability as the identified parameters is close to the corresponding physical value, whereas a value equal to 2 indicates that the parameter is 2 times higher than the corresponding physical parameter. The posterior distributions are constituted from the 4500 samples (1500 per chains).
- *neff_min, neff_min_param*
  The effective size of sample Vehtari et al. (2019) is computed for all the calibrated parameters.

Table 3: Calibrated models

		RMSE_ T_train	RMSE_ T_test	RMSE_ T_test_regul	RMSE _P_test_regul (% of Pmax)	neff_ min	neff_min _param	The normalised mean calibrated values Rg	Rg_rate	Rt	Rv
1	R4C2	0.57	0.74	1.40	18%	3375	Cm	0.64			
2	R6C3	0.78	1.03	2.90	44%	1243	Rf	0.10			
3	R5C2	0.36	0.49	1.08	14%	16	Rw			0.72	1.07
4	R5C2	0.35	0.49	1.08	14%	171	Rg_rate	0.91	1.25		
5	R5C2	0.37	0.50	1.04	14%	4097	Ci	0.93			
6	R7C3	0.44	0.61	0.62	9%	14	Rw			2.36	0.73
7	R7C3	0.44	0.61	0.61	9%	295	Rg	0.95	0.30		
8	R7C3	0.47	0.64	0.71	12%	871	Ci	0.88			
9	ISO	0.50	0.64	0.70	4%	6	Rv			1.89	0.78
10	ISO	0.50	0.63	0.70	4%	2856	Rg_rate	0.89	0.20		
11	ISO	0.52	0.67	0.70	4%	4245	Cm	0.92			

A minimum number of effective samples (200 for example) is required for having a consistent estimate of a probability distribution. Neff_min is the minimum value and neff_min_param refers to the corresponding calibrated parameter.

- *RMSE_T_train*
  It represents the Root Mean Square Error (RMSE) of the mean posterior predictive of temperature sampled on the training period (ppm_train).

$$RMSE\_T\_train = \sqrt{\frac{\sum_{n=1}^{N}(ppm\_train_n - data\_T\_train_n)^2}{n}} \quad (3)$$

- *RMSE_T_test*
  It represents RMSE of the mean posterior predictive of temperature sampled on the testing period (ppm_test).

$$RMSE\_T\_test = \sqrt{\frac{\sum_{n=1}^{N}(ppm\_test_n - data\_T\_test_n)^2}{n}} \quad (4)$$

- *RMSE_T_test_regul, RMSE_P_test_regul*
  It indicates RMSE of the mean posterior predictive of temperature (ppm_T_test_regul) and power (ppm_P_test_regul), sampled on the testing period with a temperature setpoint as input. An algorithm of perfect regulation is used.

$$RMSE\_T\_test\_regul = \sqrt{\frac{\sum_{n=1}^{N}(ppm\_T\_test\_regul_n - data\_T\_test_n)^2}{n}} \quad (5)$$

$$RMSE\_P\_test\_regul = \sqrt{\frac{\sum_{n=1}^{N}(ppm\_P\_test\_regul_n - data\_P\_test_n)^2}{n}} \quad (6)$$

Results

Table 3 presents the results obtained from the calibration of the 11 models presented previously. First, we can notice that the global resistance is correctly identified for all the models (between 5 and 10% of error), except for the models 1 and 2. This highlights the need of considering a branch without thermal capacity. Contrary to Rg, the parameters Rg_rate, Rw and Rv are not well identified. This can be a consequence of a low number of effective samples. In such cases, the sampled probability distribution is not representative of the true distribution, thus, the mean of the distribution is not a good estimate; the result is not consistent. This situation occurs for the models where Rv and Rw are calibrated (models 3, 6 and 9). For these cases, the parameters Rv and Rw turn out be highly correlated which leads to a very low value of effective samples. This correlation is illustrated in Figure 3.
Then, using Rg_rate and Rg instead of Rv and Rw fixes this problem; the models 4, 7 and 10 present a higher number of effective samples. For the models 5, 8 and 11, Rg_rate and Rw_rate are fixed, the parameters are thus hardly correlated; no problems of convergence are observed. Although the models 4 and 7 show consistent results for the parameter Rg_rate, the values remain different from the theoretical value (25% to 70% of error). We can conclude that Rv and Rw cannot be identified with the models and the data considered here.
At this stage, calibrating Rg_rate with a Bayesian method might not be pertinent since no informative prior probabilities can be used, a higher number of samples is required, and it does not significantly

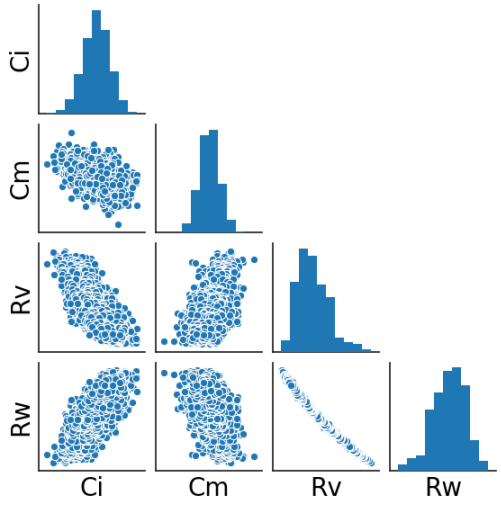

Figure 3: Pairwise relationships in the posterior distributions of model 3

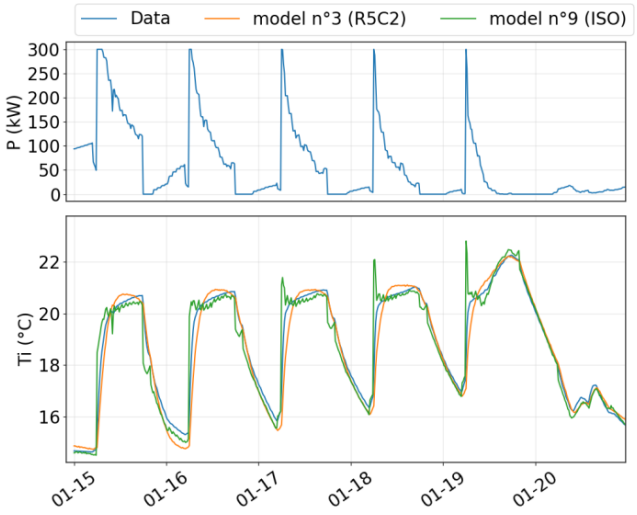

Figure 4: Simulated interior temperature for the models 5 and 11 during the training period and data of energy consumption and interior temperature issued from TRNSYS

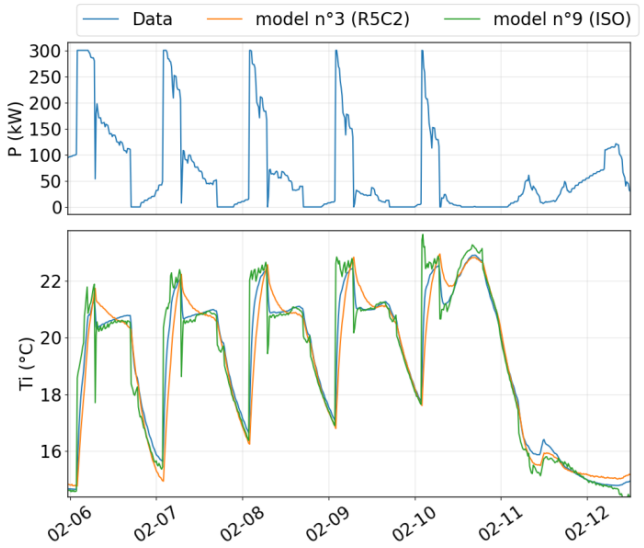

Figure 5: Simulated interior temperature for the models 5 and 11 during the testing period and data of energy consumption and interior temperature issued from TRNSYS

improve the fitting properties. The models presenting the best fitting properties for both the training and the testing data are the models of type R5C2. However, considering a set-point temperature in entry and a perfect regulation, the models ISO show a better performance for predicting both the power and the temperature. The interior temperature simulated by the model variants 5 and 11, and the input data of power and temperature are plotted in Figure 4 and Figure 5, for the first week of training period and the first week of testing period, respectively.

Conclusion

In order to efficiently calibrate RC models with Bayesian framework, the link between the parameters of the RC models and the physical parameters of the buildings needs to be well understood. Through multiples comparisons of calibrated parameters of RC models, with respect to the expected physical parameters, this paper proposes a selection of robust RC models where the global resistance of the RC model can be assimilated to the physical global resistance. A re-parametrisation of the models is successfully proposed to avoid correlation between the parameters and convergence issues. However, at this stage, only the global resistance can be safely related to the physical properties. According to these results, in the context of district model calibration, the knowledge concerning the global resistance of the buildings can be used to define informative prior probabilities. Further studies will be required in order to consistently identify the resistance related to windows and infiltration Rv, and the thermal capacities. This study should be extended to other types of buildings (residential, commercial), other sets of training and testing data. It would be also of interest to test incomplete and biased data and solicitations.

Acknowledgement

The work presented has been funded by Efficacity (The Urban Energy Transition Institute). The authors gratefully acknowledge this support.

References

Alessandrini, J., E. Fleury, S. Filfli, and D. Marchio (2003). Quelles solutions pour des bâtiments tertiaires climatisés à moins de 100kWh/m^2/an ? Rapport intermédiaire 1: Description des

bâtiments types. Technical report.

Berthou, T., B. Duplessis, P. Rivière, P. Stabat, D. Casetta, and D. Marchio (2015, dec). SMART-E: A TOOL FOR ENERGY DEMAND SIMULATION AND OPTIMIZATION AT THE CITY SCALE.

Berthou, T., P. Stabat, R. Salvazet, and D. Marchio (2014). Development and validation of a gray box model to predict thermal behavior of occupied office buildings. *Energy and Buildings 74*, 91–100.

Brastein, O., D. Perera, C. Pfeifer, and N. Skeie (2018, Jun). Parameter estimation for grey-box models of building thermal behaviour. *Energy and Buildings 169*, 58–68.

EVO (2010). Protocole International de Mesure et de Vérification de la Performance énergétique Concepts et options pour l'évaluation des économies d'énergie et d'eau Volume 1. Technical report.

Fonseca, J. A., T.-A. Nguyen, A. Schlueter, and F. Marechal (2016, feb). City Energy Analyst (CEA): Integrated framework for analysis and optimization of building energy systems in neighborhoods and city districts. *Energy and Buildings 113*, 202–226.

Harb, H., N. Boyanov, L. Hernandez, R. Streblow, and D. Müller (2016). Development and validation of grey-box models for forecasting the thermal response of occupied buildings. *Energy and Buildings*.

Hedegaard, R. E. and S. Petersen (2017). Evaluation of Grey-Box Model Parameter Estimates Intended for Thermal Characterization of Buildings. In *Energy Procedia*.

IEA (2020, Mar). Buildings Topics https://www.iea.org/topics/buildings.

Madsen, H. and J. Holst (1995). Estimation of continuous-time models for the heat dynamics of a building. *Energy and Buildings 22*(1), 67–79.

Martin, O. (2018). *Bayesian Analysis with python (Second Edition)*.

Neal, R. M. (2003). Slice Sampling. *The Annals of Statistics 31*(3), 705–767.

Raillon, L. and C. Ghiaus (2018). An efficient Bayesian experimental calibration of dynamic thermal models. *Energy 152*, 818–833.

Reynders, G., J. Diriken, and D. Saelens (2014). Quality of grey-box models and identified parameters as function of the accuracy of input and observation signals. *Energy and Buildings*.

Roujol, S., E. Fleury, D. Marchio, J. R. Millet, and P. Stabat (2003). Testing the energy simulation building model of Consoclim using BESTEST method and experimental deta, CSTB. (December 2014), 1131–1138.

Vehtari, A., A. Gelman, D. Simpson, B. Carpenter, and P.-C. Bürkner (2019, mar). Rank-normalization, folding, and localization: An improved R for assessing convergence of MCMC.

Wang, Z. and Y. Chen (2019, nov). Data-driven modeling of building thermal dynamics: Methodology and state of the art. *Energy and Buildings 203*, 109405.

Wang, Z., Y. Chen, and Y. Li (2019, jul). Development of RC model for thermal dynamic analysis of buildings through model structure simplification. *Energy and Buildings 195*, 51–67.